JOURNAL OF APPLIED ELECTROCHEMISTRY 9 (1979) 219–232

On the electrodeposition of hard gold

H. ANGERER*, N. IBL

Swiss Federal Institute of Technology, Zurich, Switzerland

Received 15 June 1978

The electrodeposition of hard gold in layers of 2 μm was investigated. The electrolyte was an acid citrate bath (pH 3·5) with cobalt as an additive. A flow cell allowed a controlled variation of the hydrodynamic conditions. The following features were examined quantitatively in the experiments: the current efficiency for gold deposition (10–30%), the carbon and cobalt content, as well as the porosity of the deposits, and the morphology [by scanning electron microscope (SEM)]. Above 50 mA cm^{-2} the deposition of gold and to a minor extent the incorporation of cobalt become mass transport limited (with certain complications resulting from the complex nature of the diffusion layer). The influence observed below 50 mA cm^{-2} seems to be due to the synergic effect of the transport controlled reduction of dissolved oxygen. A simple qualitative model for the incorporation of carbon is proposed. The substantial decrease in current efficiency observed upon the addition of cobalt to the bath is probably caused *both* by a decrease of the hydrogen overpotential and by an increase of the overpotential for gold deposition. From the viewpoint of technical application, the most relevant result, is the substantial decrease in porosity at decreasing current density (c.d.) and increasing flow rate.

Nomenclature

c_e	interfacial concentration (mol m^{-3})
c_0	bulk concentration (mol m^{-3})
D	diffusion coefficient (m^2 s^{-1})
D_h	hydraulic diameter (m)
F	Faraday's constant (96 500 C equiv.$^{-1}$)
j_{Au}	partial c.d. of gold deposition (A m^{-2})
j_{Co}	partial c.d. of cobalt deposition (A m^{-2})
j_L	limiting c.d. for gold deposition (A m^{-2})
j_H	partial c.d. for hydrogen evolution (A m^{-2})
j_t	total c.d. $\approx j_{Au} + j_H$ (A m^{-2})
$j_{H_3O^+}$	c.d. defined by Equation 7
k_{exp}	experimental mass transfer coefficient (m s^{-1})
k_g	mass transfer coefficient for gas stirring alone (m s^{-1})
k_t	overall mass transfer coefficient (m s^{-1})
k_v	mass transfer coefficient for stirring by hydrodynamic flow alone (m s^{-1})
v	flow velocity of solution (m s^{-1})
z	charge number of electrode reaction (equiv. mol^{-1})
ν	kinematic viscosity (m^2 s^{-1})
ω	angular velocity (rad s^{-1})
(Re)	Reynolds number vD_h/ν
(Sc)	Schmidt number ν/D
(Sh)	Sherwood number kD_h/D

1. Introduction

It is estimated that 121 tons of gold were electrodeposited in the world in 1970 for application in electronics [1]. The improvement of the properties of these deposits or the possibility of retaining the desired specifications with thinner deposits is of great practical importance. Numerous studies have been devoted to this problem (for a review see [2–4]). Recently, pulse electrolysis has also been applied. In our laboratory a systematic study with this method was made. The results have been briefly reported in [6] and will be discussed in more detail in a later communication [7]. To facilitate the interpretation of the measurements, they were carried out under controllable hydrodynamic conditions, allowing a quantitative treatment of mass transport. To achieve a valid comparison with d.c. experiments the latter should be carried out with similar precautions. We have thus studied first certain aspects of the electrodepo-

* Present address: Diamond Shamrock Electrosearch SA, 1227 Carouge, Switzerland.

sition of gold with d.c. under controllable hydrodynamic conditions. The results are reported in this paper.

An acid citrate solution with addition of cobalt was used. This is one of the most commonly employed baths in gold plating. Several authors have reported that the deposits contain considerable amounts of foreign material (carbon, cobalt, hydrogen, oxygen etc.). In the present study we investigated, as a function of current density and hydrodynamic flow rate, the carbon and cobalt contents as well as a practically important property, the porosity. Further, the morphology of the gold coating was investigated by a scanning electron microscope (SEM).

2. Experimental technique

2.1. *Electrolytic cell*

The flow cell is sketched on Fig. 1. The solution flow velocity through a channel of 70 cm length was adjusted from 30–150 cm s^{-1}. The dimensions of the cross-section were 2 x 0·5 cm, the entrance length was 40 cm. The solution was recycled through a circuit including a thermostat, a rotameter, a filter and a pump. The cell and the circuit were constructed from hard PVC and glass, respectively. The two electrodes were 14 cm in length (in the direction of the stream) and 2 cm in breadth (thus completely covering the channel width). They were 0·5 cm apart. This arrangement

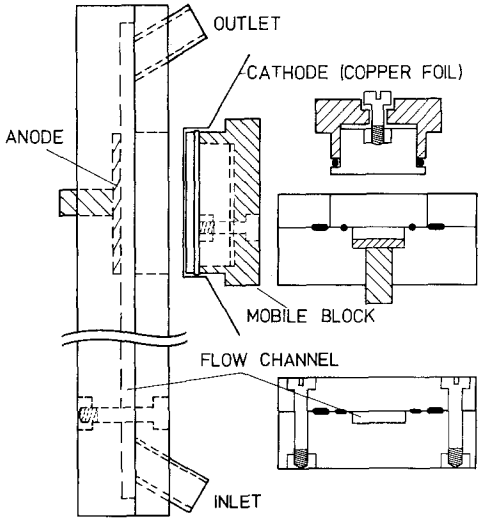

Fig. 1. Electrolytic flow cell.

ensures defined hydrodynamic conditions as well as a uniform primary and secondary current distribution. The uniformity of the coating thickness was checked by means of a betascope.

The anode was of platinized titanium, the cathode was a 50 μm thick foil of bright copper supported by the mobile block. It was made electrolytically and prepared as follows. The foil was first dipped into a 1·5 M KCN solution and rinsed with water. Then it was cathodically degreased in a commercial bath (Enbond 160) at 60° C and a current density of approximately 150 mA cm^{-2}. Finally it was etched with 5 M HCl and thoroughly rinsed with distilled water.

The block with the cathode could be inserted into the cell and tightened rapidly so that the cleaned electrode had no time to dry up before it came into contact with the plating solution. All experiments were carried out under constant current conditions. The temperature was kept at 27° C ± 0·5° C.

2.2. *Plating solution*

The composition of the electrolyte was:

$KAu(CN)_2$	15 g dm^{-3}
Citric acid	50 g dm^{-3}
Cobalt (added as acetate)	0·07 g dm^{-3}
pH (adjusted with KOH)	3·5

Unless otherwise indicated all experiments were carried out with this solution, which will be referred to as the DUOR bath. Upon use the bath ages and becomes yellow. According to the literature [8] this is due to the formation of $[Co(CN)_6]^{3-}$ which does not react at the cathode. The solution was renewed after the gold content had dropped to 95% of its original value. No significant colour change was observed within this period.

To ascertain that the ageing of the solution does not vitiate the results two sequences of experiments were usually carried out, one at increasing, the other at decreasing current density.

2.3. *Measurement procedures*

2.3.1. The carbon content. The carbon content of the deposit was determined by combustion, and thus converting the carbon to CO_2 which was measured by coulometric titration [9].

2.3.2. The cobalt content. The cobalt content was measured by atomic absorption spectroscopy.

2.3.3. The current efficiency. The current efficiency for gold deposition was determined by weighing the deposit before and after plating.

2.3.4. The porosity. The porosity was determined with the SO_2 test [10, 11]. In this technique the deposit is exposed during 24 hours to an atmosphere of 10% SO_2 which is formed by a slow chemical reaction of sulphuric acid with sodium thiosulphate. The transversal pores appear as sharp brown spots which can be counted.

2.3.5. Morphology. To investigate the morphology of the deposits pictures were taken with a scanning electron microscope.

The experimental technique and the results obtained are described in more detail in [12].

3. Mass transport considerations and measurements

The mass transport characteristics of the flow system were tested in the usual way [13] by measuring the limiting current of the reduction of ferricyanide at a nickel cathode in a KOH solution. The flow velocity was varied from 30–150 cm s^{-1}, (corresponding to Reynolds numbers, (*Re*), of 2900–13 400 based on the hydraulic diameter) and was within the turbulent range. The results were in good agreement with the correlation proposed by Pickett and Ong [14]:

$$(Sh) = 0{\cdot}023(Re)^{0{\cdot}8}(Sc)^{1/3}. \qquad (1)$$

For our gold plating bath (see Section 2.2) the kinematic viscosity ν at 27° C was 0·009 16 cm^2 s^{-1}.

The diffusion coefficient D of the gold species was determined with a rotating disc cathode. However, owing to the hydrogen evolution, no limiting current plateau was discernible. Another method, used by Cheh [15] was thus followed. A current substantially higher than the limiting current was applied and the deposit obtained on a platinum disc after a certain time of deposition was anodically redissolved in 0·1 M KCN solution*; the amount of electricity needed for the redissolution yielded, upon division by time, the average limiting c.d. of gold deposition, j_L. The diffusion coefficient can then be calculated from the classical relationship [16]

$$j_L = 0{\cdot}62zFD^{2/3}c_0\nu^{-1/6}\omega^{1/2} \qquad (2)$$

where the charge number of the electrode reaction z is equal to one. A plot of j_L against $\omega^{1/2}$ yielded a line which was not straight and the extrapolation of which crossed the ordinate at a value of j_L substantially larger than zero. This behaviour can possibly be explained by the relatively intense hydrogen evolution during the gold deposition. Two effects arise from this: (a) the acceleration of mass transport (however, this influence decays at high rotation speeds) (b) the hydrogen bubbles block part of the surface, thus decreasing the measured j_L. The measurements made at the highest and lowest speeds used (100 and 10 rev s^{-1}), yielded D values of 0·50 and 1·2 × 10^{-5} cm^2 s^{-1}, respectively. In view of this scatter in the results further measurements were made with a more diluted gold bath used by Cheh [15] similar to ours [$KAu(CN)_2$ 1·3 g dm^{-3}, $(NH_4)_2HC_6H_5O_7$ 50 g dm^{-3}, pH 5]. The deposition and dissolution current densities were 16 and 6 mA cm^{-2}, respectively. The hydrogen evolution was thus less intense and indeed the plot of j_L versus $\omega^{1/2}$ was now a straight line going through the origin and yielding a diffusion coefficient of 0·74 × 10^{-5} cm^2 s^{-1} at 27° C. This is in good agreement with the value of 1·67 × 10^{-5} cm^2s^{-1} reported by Cheh [15] for 60° C if we assume a typical temperature coefficient of 2.5% per degree. However, our results are at variance with the data of Kekovskii *et al.* [17] who obtained with the porous cup method 1·6 × 10^{-5} cm^2 s^{-1} at 25° C for infinite dilution. This discrepancy may be linked with the complex nature of the diffusion layer in our system.

The presently accepted view [8] is that the gold complex predominating in baths of the acid citrate type, like ours, is $Au(CN)_2^-$. However, according to Harrison and Thompson [18] and to Burrows *et al.* [19] the electrode reaction involves the adsorption of AuCN i.e. the homogeneous pre-reaction

$$Au(CN)_2^- \longrightarrow Au(CN) + CN^- \qquad (3)$$

takes place in the diffusion layer. Further CN^- ions

* The deposition c.d. was 250 mA cm^{-2} and the dissolution c.d. 6 mA cm^{-2}.

are liberated by the reduction of Au(CN) at the cathode. These CN^- ions react with the protons of the buffer

$$H_3O^+ + CN^- \rightleftharpoons HCN + H_2O. \quad (4)$$

The diffusion layer is thus depleted with respect to gold and enriched with respect to CN^-. Further, owing to the hydrogen evolution the citric acid concentration tends to be lower and the pH higher near the electrode than in the bulk electrolyte.

The diffusion coefficient measured is thus an effective value [20] which represents some average of the values for $Au(CN)_2^-$ and Au(CN). Even if Reactions 3 and 4 are at equilibrium (i.e. if the diffusion layer is at equilibrium) there is a shift in the concentration ratio $Au(CN)_2^-/Au(CN)$ across the diffusion path. Even at a given bulk concentration there may thus be some variation of D depending on the circumstances. It is thus best to use effective diffusion coefficients measured under conditions as close as possible to those at hand [20]. In our case this means that values measured with a rotating disc electrode are expected to be better suited than those obtained by the porous cup method. In the following calculation we will use the value of $0{\cdot}74 \times 10^{-5}$ cm^2 s^{-1} obtained with the electrolyte used by Cheh; this value is between the scattered results measured in the DUOR bath under concomitant strong hydrogen evolution.

With this diffusion coefficient one obtains for our flow cell from Equation 1 mass transfer coefficients k_v of 0·001 34 and 0·0046 cm s^{-1} for Reynolds numbers of 2900 and 13 400, respectively. In addition to this calculation, which disregards the influence of gas stirring, the latter must be evaluated. The mass transfer coefficient due to hydrogen evolution in acid solutions, k_g, can be calculated from a correlation given by Ibl and Venczel [21, 22]. We assume a degree of surface coverage by the gas bubbles of 0·2 and an average bubble diameter of 0·35 mm [21, 22]. The current efficiency for gold deposition was between 10–30% (Fig. 4a). We thus calculate k_g for an average current efficiency for hydrogen evolution of 75% and obtain for total c.d.'s, j_t, of 10 and 150 mA cm^{-2} k_g values of 0·0008 and 0·0031 cm s^{-1}, respectively. In the low c.d. range of this study k_g is substantially smaller than k_v and does not strongly influence the mass transport, especially at the high flow rates. However, in the high c.d. range k_g is of the same order as k_v or even larger. Under these conditions an accurate calculation of the mass transport rate is not possible. Approximate correlations allowing an estimate of the overall mass transport coefficient k_t under concomitant stirring by gas evolution and by a hydrodynamic flow have been given. We use the relationship [23]

$$k_t = (k_v^2 + k_g^2)^{1/2} \quad (5)$$

and obtain for the mass transport coefficients of gold deposition in our flow cell the values given in Table 1. The agreement between the calculated and the observed values for k_t can be regarded as fair. It is also of interest to estimate the change in pH across the diffusion layer, which occurs due to the liberated cyanide ions when the gold complex is discharged and due to the deposition of hydrogen, i.e.

$$CN^- + H_3O^+ \rightleftharpoons HCN + H_2O \quad (4)$$

and

$$2H_3O^+ + 2e^- \rightleftharpoons H_2 + 2H_2O. \quad (6)$$

The consumption of protons originating from the

Table 1. Calculated and experimental overall mass transfer coefficients (cm s^{-1}) for gold deposition. The figures in parenthesis are the experimental values derived from the plateaus of Fig. 5a (see Section 5)

(*Re*)	k_t ($j_t = 10$ mA cm^{-2})	k_t ($j_t = 150$ mA cm^{-2})	k_{exp} ($j_t = 150$ mA cm^{-2})
2900	0·0015	0·0034*	(0·0023)*
6550	0·0026	0·0042	(0·0039)
9650	0·0036	0·0047	(0·0054)
13 400	0·0047	0·0055	(0·0066)

* k_t and k_{exp} for 100 mA cm^{-2} (no experiments at 150 mA cm^{-2} were made due to powder formation).

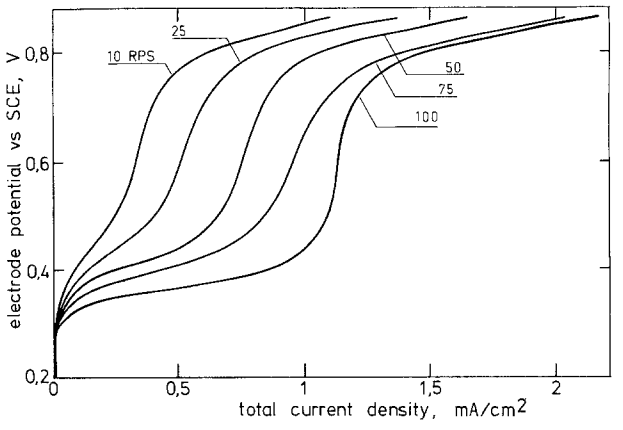

Fig. 2. Total current potential curve at rotating copper disc for various speeds of rotation.

citric acid can thus be described in terms of a c.d. $j_{H_3O^+}$:

$$j_{H_3O^+} = 2j_{Au} + j_H. \qquad (7)$$

Owing to the relatively small dissociation constants of the citric acid (pK_a 3·1, 4·8 and 5·4 at 25° C) we may approximate the supply of protons to the cathode by considering only their transport as undissociated acid. In view of the approximative character of the calculation it is further justified to assume the same diffusion coefficient for citric acid as for the gold species (a value of $0{\cdot}65 \times 10^{-5}$ cm^2 s^{-1} for a 0·23 M solution of citric acid at 18° C is given in the literature [24]). We thus can calculate k_t of the citric acid in the same way as we have done for gold in Table 1.

We assume all homogeneous reactions involved such as Reaction 4 to be fast compared to diffusion. The interfacial concentration c_e can be computed from the relationship:

$$c_e/c_0 = 1 - j_{H_3O^+}/zFc_0k_t \qquad (8)$$

where $j_{H_3O^+}$ is defined by Equation 7. One finds that c_e/c_0 varies between 0·31–0·96 for j_t values of 100 mA cm^{-2} [$(Re) = 2900$] and 10 mA cm^{-2} [$(Re) = 13\,400$], respectively.

It can thus be said that at c.d.'s up to 10 mA cm^{-2} there is no significant change in pH across the diffusion layer. In the case of high c.d. there might be a considerable increase of the pH in the vicinity of the electrode, leading to a strong influence on the deposition characteristics. Several authors reported that an increase of the pH in the plating bath decreases the cobalt content of the deposit and virtually eliminates the cobalt if the pH exceeds a value of ~ 5·5 [8, 32].

4. Current–voltage curves

Fig. 2 shows total current–potential curves in the region of low d.c. They were taken with a rotating disc electrode at various speeds of rotation using a continuously increasing current at a scanning rate of 1 mV s^{-1}. To investigate whether the limiting current plateaus are due to the reduction of dissolved oxygen or to the diffusion controlled discharge of a cobalt species, current–potential curves

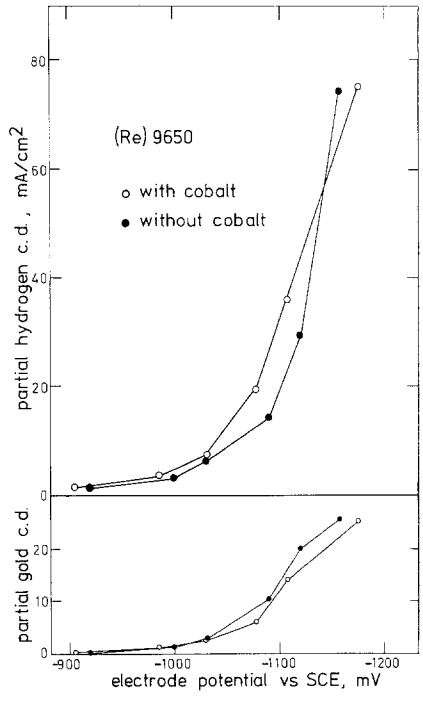

Fig. 3. Partial current density– potential curves for gold and hydrogen discharge in the DUOR bath with and without Co additive.

were taken in a solution with tenfold increased cobalt concentration (0·69 g dm^{-3}). No significant change of the height of the plateau was observed. This, together with the fact that the plateaus disappeared when the oxygen was removed by bubbling nitrogen through the solution gives strong evidence for oxygen discharge being responsible for the limiting current plateaus.

The reduction of oxygen governed by mass transport explains the decrease in current efficiency for the gold deposition with increasing Reynolds numbers in the low c.d. range (see Section 7.3.4). Fig. 3 shows the partial current density–potential curves for gold and hydrogen discharge, respectively. They were obtained by measuring the cathode potential (with a Luggin capillary against a reference electrode) at a given total current density j_t and by determining the current efficiency for gold from the weight difference before and after plating.* It was assumed that the partial c.d. for hydrogen discharge can be expressed as $j_H = j_t - j_{Au}$. The figure provides a comparison between the behaviour of the DUOR bath with and without cobalt additive.

5. Current efficiency and rate of metal deposition

Fig. 4a shows the current efficiency of gold deposition as a function of total c.d. for various flow velocities. Curves going through a maximum were also obtained for a DUOR bath without cobalt additive but the current efficiencies were much higher, especially in the low c.d. range. Fig. 4b shows the current efficiency as a function of flow rate for a bath with cobalt. From the measured current efficiency the rate of gold deposition was calculated and plotted in Fig. 5b as a function of flow velocity. The various curves correspond to various total current densities. Very similar curves were obtained for a DUOR bath without cobalt.

The knowledge of the current efficiency

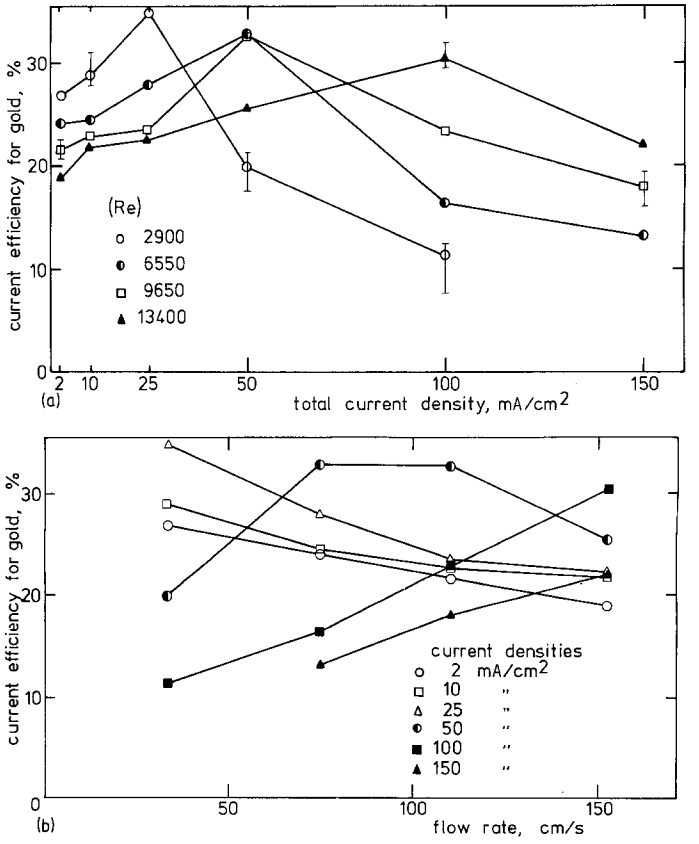

Fig. 4(a) Current efficiency as a function of total current density. (b) Current efficiency as a function of flow velocity.

* Unpublished experiments of Dr J. Bielinski (Warsaw Technical University, Poland) carried out in our laboratory.

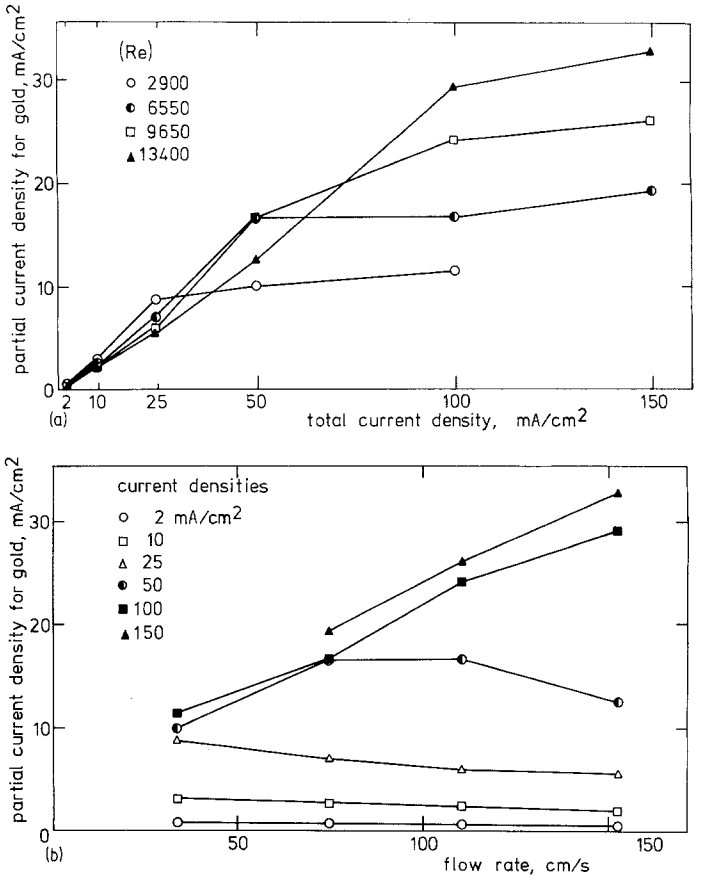

Fig. 5. (a) Partial current density of gold deposition as a function of total current density. (b) Partial current density of gold deposition as a function of flow rate.

allowed the adjustment of the duration of the galvanostatic electrolysis in such a way that deposits of the same thickness (2 μm) were obtained for all experiments in the following section.

The figures show the average current efficiencies and carbon contents for 5 and 3 measurements, respectively.

6. Measurements of porosity and of the incorporation of foreign substances

On Fig. 6 is plotted the porosity as a function of flow velocity for various total current densities. Figs. 7 and 8 show the carbon and cobalt contents of the deposit as a function of total current density for different flow velocities. All the quantities measured depend markedly on both variables studied, c.d. and (*Re*). The curves for the carbon and cobalt contents exhibit a maximum which is reached at increasing c.d.'s with increasing flow velocity. The carbon contents are remarkably high.

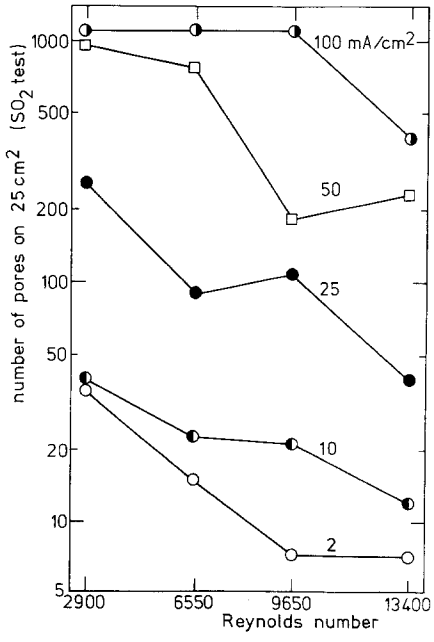

Fig. 6. Porosity as a function of (*Re*).

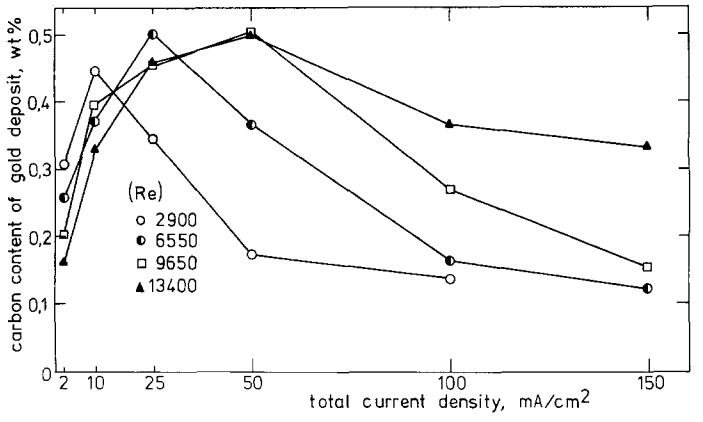

Fig. 7. Carbon content of deposit (wt%) as a function of total current density.

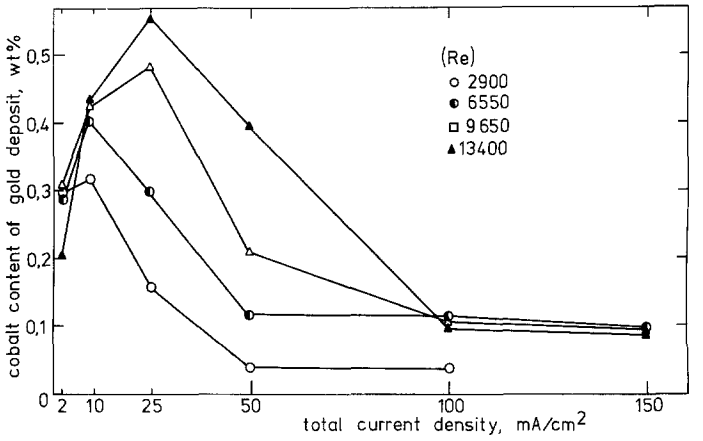

Fig. 8. Cobalt content of deposit (wt%) as a function of total current density.

The largest observed value, expressed in mol% C/Au is 8%. The highest cobalt content is about 2 mol% as compared to a molar ratio of cobalt-to-gold in the solution of 0·023.

From the viewpoint of the properties of the electroplate the amount of foreign material in the deposit is of importance. However, in the context of a comparison with mass transport theory the relevant quantity is the rate of incorporation of cobalt and carbon, i.e. their interfacial flux densities in the solution. These rates were calculated from the amount of Co and C contained in the deposit. The results are plotted in Figs. 9 and 10 as a function of total c.d. and flow velocity, respectively.

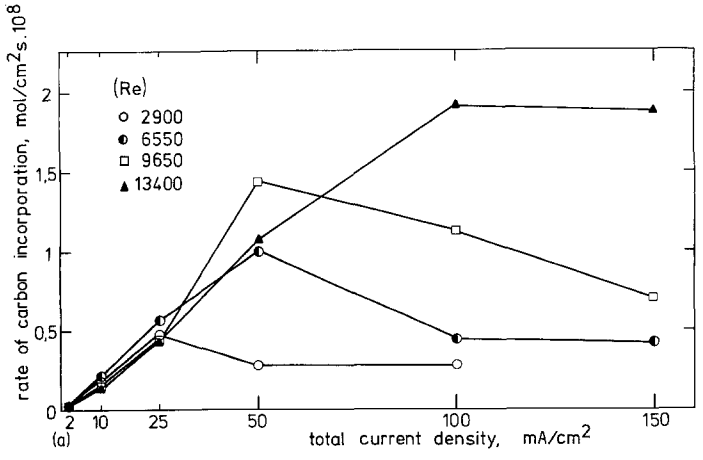

Fig. 9. (a) Rate of incorporation of C as a function of total current density. (b) Rate of carbon incorporation as a function of flow rate.

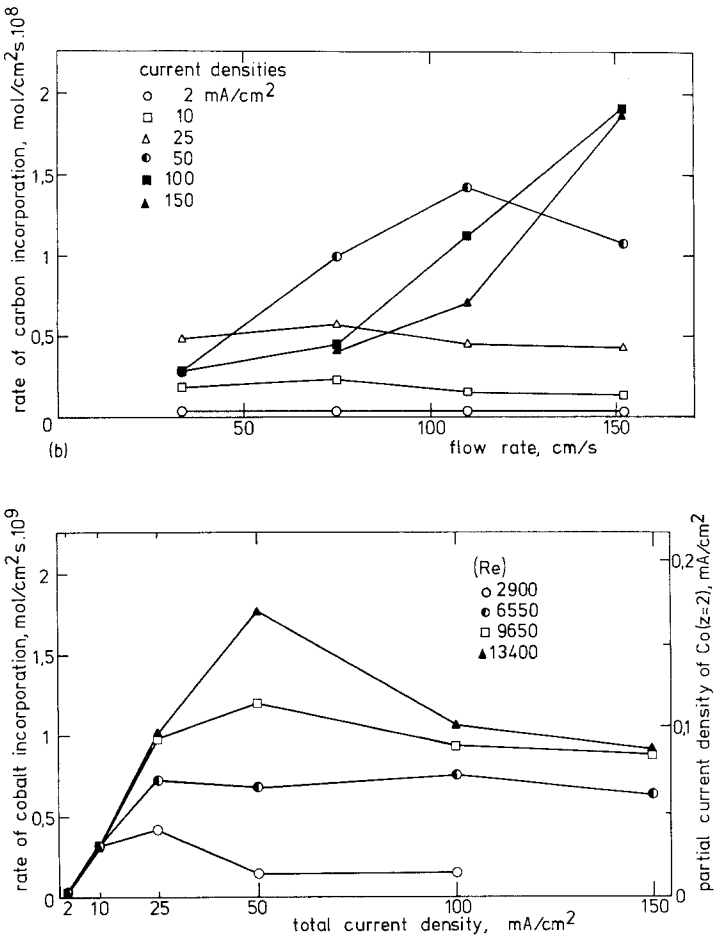

Fig. 10. Rate of incorporation of cobalt as a function of total current density.

7. Discussion

7.1. *Comparison with results of other authors*

The porosity of gold deposits has been studied by Clarke [25, 26] for solutions different from ours. The dependence on c.d. exhibited a minimum whereas in our case the porosity steadily decreases with decreasing c.d. Similar results to ours were obtained by Ashurst and Neale [27]. They also found the least porosity at low c.d. and high agitation rate. Early measurements of the quantity of carbon present in gold electroplates were made by Egan [28] and Munier [29]. Detailed studies of the carbon and cobalt contents were made by Holt *et al.* [30–32] and Knödler [8]. The latter also measured the amount of incorporated hydrogen, nitrogen and oxygen. The content of all these foreign substances in the deposit markedly increases if cobalt is present in the solution.

The cobalt and carbon content was found to substantially depend on the pH of the plating solution, on the temperature, and on the c.d. Experiments on the influence of stirring were performed by Holt *et al.* [30] but no systematic study was made. The results of the present work show that the intensity of agitation is a further important variable.

Holt *et al.* [30] and Knödler [8] found for an acid citrate bath (pH 3·5–4) that the carbon content plotted as a function of c.d. goes through a maximum at about 10–20 mA cm^{-2}. This is in agreement with our findings (Fig. 9) for a flow velocity of 30 cm s^{-1} [$(Re) = 2900$] where the intensity of agitation was probably close to that prevailing in the baths of the aforementioned authors, in which stirring was due to hydrogen evolution only (see Section 3). The carbon contents at the maximum reported by Knödler [8] and Holt [30] (0·3 and 0·2 wt%, respectively) are

somewhat smaller than our value (0·45 wt%), but the order of magnitude is the same and it is to be noted that the concentrations of the bath were somewhat different from ours. In particular, the cobalt content of Knödler's bath was substantially higher than ours (0·5 against 0·07 g dm^{-3}) but according to this author's findings the carbon content of the deposit varies little with cobalt concentration in baths higher than 0·1 g dm^{-3}.

The drop in current efficiency observed by us at high c.d. had also been reported by Holt and Stanyer [31] and Holt [32]. On the other hand, Knödler, like ourselves (Fig. 8) has found a maximum in the plot of cobalt content versus c.d. at about 10–20 mA cm^{-2} (Fig. 6 in [8]). The numerical value measured by him (Fig. 9 of [8]) at 10 mA cm^{-2} with a bath containing 0·1 g dm^{-3} cobalt (but somewhat less gold than ours) was smaller than our result (0·22 against 0·32 wt% at $(Re) = 2900$). By and large, however, it can be said that inasmuch as the results are comparable there is a fair agreement between our measurements and those of Holt *et al.* and of Knödler.

7.2. *Influence of codeposition of cobalt on hydrogen evolution*

Both our results and those of Knödler [8] have shown that the current efficiency of gold deposition substantially decreases when cobalt is added to the bath. The actual differences in overpotential (Fig. 3) are small and are not much outside of the reproducibility limits of the experiments. It still seems that the decrease in current efficiency through the cobalt additive is caused by the fact that the hydrogen overpotential decreases whereas that for gold deposition increases. The latter may be due to an inhibition of the crystallization by carbon, the incorporation of which is greatly enhanced by the cobalt additive. We will return to this topic in a later paper [7] where we will discuss the peculiarities of the morphology of the deposits obtained by pulse electrolysis.

The inhibition of electrocrystallization in general is a well-known phenomenon which has been reviewed comprehensively by Fischer [43].

7.3. *Mass transport effects*

7.3.1. General remarks. A striking feature of our results is the considerable influence of flow velocity, i.e. the sensitivity to mass transport. This applies to the porosity (Fig. 6), to the current efficiency (Fig. 4b) as well as to the carbon and cobalt contents (Fig. 7 and 8) and to their incorporation and deposition rates (Figs. 9 and 10). Except, perhaps, for porosity one can roughly distinguish two current density ranges above and below 50 mA cm^{-2}. In the high c.d. range the influence of the mass transport rate is very marked and moreover it acts in a direction opposite to that observed in the low c.d. range. We will discuss in turn the transport effects in the two cases.

7.3.2. Current efficiency and gold deposition in the high current density range. At high c.d. the current efficiency for the discharge of gold drops (Fig. 4a). This appears to be due to the limitation of the rate of gold deposition by mass transport. Indeed, the plot of the partial c.d. j_{Au} versus total c.d. j_t exhibits a plateau, the height of which increases with increasing rate of hydrodynamic flow (Fig. 5a). This height was expressed as a mass transfer coefficient k_{exp} and compared with the calculated values k_t in Table 1. The agreement can be regarded as fair, if we remember the uncertainty of the theoretical evaluation due to the concomitant gas evolution (see Section 3). In view of this uncertainty and further because of the shift in the ratio k_{exp}/k_t it cannot be neglected that kinetic effects are involved to some extent in the determination of the rate of gold deposition but essentially the latter appears to be mass transport controlled in the high c.d. range. This is confirmed by the fact that the height of the limiting current plateau is virtually the same for baths with and without cobalt additive. The slight slope of the plateaus can be explained by the fact that with increasing c.d. the rate of hydrogen evolution increases and thus causes some increase of the mass transfer coefficient. However, in the plateau region the mass transport rate for gold increases much more slowly than the rate of gas evolution which explains the decrease of current efficiency observed at high c.d.

In general at the limiting current of metal deposition very rough or powdery deposits are obtained [33–36]. Fig. 11 shows photographs of the electroplates below and within the limiting c.d. range taken with a scanning electron microscope. The

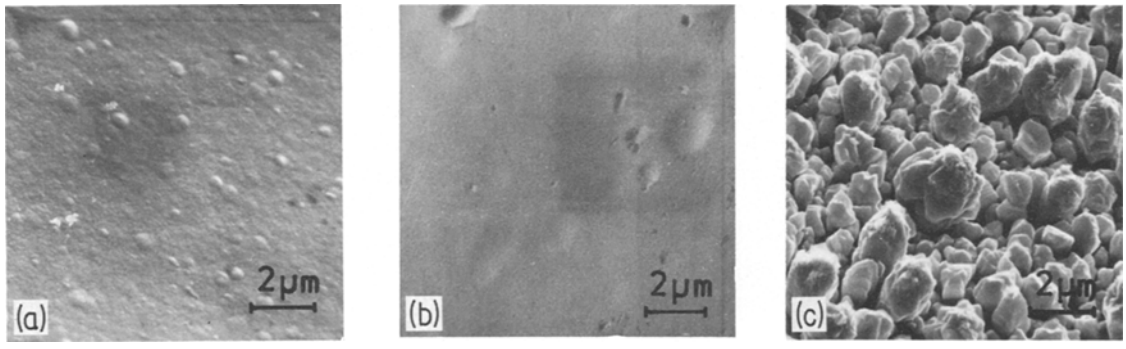

Fig. 11. SEM photographs of deposits obtained at $(Re) = 9650$: (a) $j_t = 2\,mA\,cm^{-2}$, (b) $j_t = 50\,mA\,cm^{-2}$, (c) $j_t = 100\,mA\,cm^{-2}$. Magnification ×4150.

deposit obtained at $150\,mA\,cm^{-2}$ is dull, rough and friable. The onset of the formation of a roughened deposit coincides rather sharply with the beginning of the plateau, in agreement with expectation. The porosity in the region of the plateau is very high (Fig. 6), which is not surprising in view of the morphology of the deposit.

7.3.3. Incorporation of cobalt in the high current density range. In the low c.d. range the rate of incorporation of cobalt appears to be charge transfer controlled (Fig. 10). In the higher range the rate ceases to increase with increasing c.d., i.e. with increasing overpotential. This suggests that the incorporation of cobalt now tends to be limited by mass transport. This is confirmed by the present findings and the results of Knödler [8] and Bielinski [44] * who observed a steadily increasing cobalt content with increasing cobalt concentration in the plating solution. (Similar observations were also made in pulse electrolysis).

However, a maximum is observed on the curves of Fig. 10 as well as on the curves taken at other cobalt concentrations of the plating bath [8, 44]. This seems to indicate that some complication is involved, which may be due to the complex nature of the diffusion layer. We may speculate about possible interpretations.

At increasing total c.d. j_t, the rate of hydrogen evolution becomes larger. As was shown in Section 3 in the highest c.d. range we used in this work the pH near the interface is probably substantially higher than in the bulk. This shifts towards the left the dissociation equilibrium, thereby increasing the free cyanide concentration. The latter effect favours the formation of cobalt complexes with a larger number of cyanide ligands such as $Co(CN)_6^{3-}$ which does not react at the cathode and the formation of which therefore lowers the rate of cobalt deposition. This phenomenon is particularly marked at the highest Reynolds number (Fig. 10) because then the maximum rate of gold deposition and thus of cyanide formation due to the discharge of $Au(CN)_2^-$ is largest. This liberation of cyanide ions in the diffusion layer also forces the formation of $Co(CN)_6^{3-}$.

A further possible complication is the influence of kinetic effects. Several cyanide complexes are present in the solution and the rate of supply of the reacting species by a pre-reaction may be slow compared to diffusion and decrease with increasing pH. This could also explain the decrease of the rate of incorporation of cobalt observed at high c.d. (Fig. 10). The above hypothesis would be in agreement with the following findings: Assuming a similar diffusion coefficient for the cobalt species as for gold and the analytical cobalt concentration ($0{\cdot}069\,g\,dm^{-3}$) being available for the cathodic reaction the rate of incorporation is about a factor of five less than the calculated value. This suggests that the reacting species is present in a much lower concentration compared to the analytical value, thus pointing towards a homogeneous pre-reaction with a low reaction rate. However, various other explanations are

* In this measurement where the cobalt concentration ranged from 10–2500 mg dm^{-3}, the rate of cobalt codeposition increased with the concentration of Co in the solution but somewhat slower than would correspond to a simple proportionality.

possible. Another very different explanation would be an inhibition of the cobalt deposition by the blocking of the active centres by some reaction products, produced at high overpotentials. One would then have to assume that only the cobalt and not the gold deposition is inhibited (Fig. 5).

In the above context one can explain the occurrence of a maximum in the curves showing the cobalt content as a function of c.d. (Fig. 8). Indeed, it can be inferred from Figs. 5a and 10 that the partial current–voltage curve* is steeper for cobalt (j_{Co}) than for gold deposition (j_{Au}) (i.e. the overpotential is lower) and that a limiting current is reached at less negative potentials in the case of cobalt. Therefore, the ratio j_{Co}/j_{Au} (and thus the cobalt content) increases with increasing j_t in the low, potential controlled c.d. range. On the other hand, in the range of j_t where the cobalt deposition is mainly transport controlled (but not yet that of gold), j_{Co} and therefore the ratio j_{Co}/j_{Au} at a given potential increases with increasing flow rate v, thus explaining why the maximum is the higher for the larger values of v. However, inasmuch as j_{Au} (but not j_{Co}) continues to increase with increasing j_t, the cobalt content of the deposit drops and finally reaches a value rather independent of v, when the cobalt and gold deposition are both under diffusion control (with some limitations in the case of cobalt, which were mentioned earlier in this section). One can thus indeed nearly explain the shape of the curves' cobalt content $= f(j_t)$ (at constant v) observed by us and other authors.

7.3.4. Mass transport effects in the low c.d. range. The low c.d. range extends up to about 50 mA cm^{-2}. Several curves exhibit two branches (Figs. 4b, 5b, 9b); the first belongs qualitatively to the high c.d. range, i.e. the increase of the rate of deposition with increasing flow velocity is the predominating effect, the second branch belongs to the low c.d. range, i.e. the decrease of the deposition rate with increasing v is predominating. The influence of mass transport persists even at the lowest c.d. of 2 mA cm^{-2}. In the case of incorporation and deposition rates it is quite small but probably real because the same trends are repeatedly observed (Figs. 4b, 5b, 9b, 10). It is noteworthy that this influence exists even at 2 mA cm^{-2} because then, depending on v, j_{Au} and j_{Co} amount to only 1–4·5% and 2–10% of their limiting values, respectively. Under these circumstances, except for the improbable case of a completely reversible metal deposition, the mass transport of Au and Co cannot appreciably affect the deposition rate of these metals. Moreover, the increase of v causes a decrease of j_{Au} and j_{Co}, instead of an increase as would be expected normally and as is indeed found in the range of high j_t. This suggests that the observed effects are indirect ones due to the action of a species, the reaction of which is mass transport limited down to j_t values of 2 mA cm^{-2}. In Section 4, it was shown that the reduction of dissolved oxygen is the cause of the limiting current plateaus (Fig. 2). At $j_t = 2$ mA cm^{-2} the mass transport controlled discharge of oxygen makes up for a not negligible part of the total c.d. It can thus explain the decrease of j_{Au} with increasing flow rate. At higher c.d. up to 50 mA cm^{-2} this effect may possibly be interpreted at least partly as being due to an increasing inhibition of the gold deposition by the discharged oxygen, the formation rate of which increases with increasing flow rate.

By and large from this work as well as from that of other authors, it appears that the gold bath of this study exhibits a remarkable synergy between all the investigated reactions: the deposition of gold and cobalt, the incorporation of carbon and the evolution (and incorporation) of hydrogen and oxygen (see also Section 7.4).

7.4. *Incorporation of various compounds and of carbon*

In addition to the substances already mentioned (Co, C, N, H, O) it has been found that K is also incorporated into the deposit [37, 38]. The latter then contains a variety of elements in considerable amounts. Most of them appear in the electroplate when Co is present in the solution and, further, the amounts of the incorporated materials depend on the cobalt concentration in the bath [8]. Holt and Stanyer [31] have assumed from radiotracer studies that the incorporated carbon is not built

* Primarily, the Figs. 5a and 10 represent the partial c.d. as a function of total c.d. j_t rather than of overpotential. However, j_t is related to the electrode potential, so that indirectly Figs. 5a and 10 represent current–voltage curves.

Table 2. Molar ratio of incorporated foreign substances in hard gold deposits

Reference	*C:O*	*C:N*	*C:Co*	*C:H*	*C:Au*
Malme and Vasile [37]	2·6–3·6				
Knödler [8]	5–7·7	1·25–4	0·78–4·6	0·21–0·59	0·022–0·05
This study			3·3–20·5		0·021–0·082

into the lattice but is probably situated at the grain boundaries. These facts have lead various authors to the opinion that the elements are incorporated in the form of some compound. In particular, the formation of a polymer [29, 39] such as $(HCN)_4$ or cobalt cyanide complexes [30, 40] have been envisaged. Recently, Eisenmann [41] has come to the conclusion that the incorporated compound is $KCo[Au(CN)_2]_3$. He was able to isolate this compound in solid form from the solution where it dissociates into cobalt, gold and cyanide ions. According to him the plating baths are usually operated under conditions close to the solubility limits of the above complex which consequently precipitates at the cathode. In our opinion the precipitation would be more likely in the bulk of the solution than at the interface, because in reality the diffusion layer is depleted with respect to cobalt and gold. Above 50 mA cm^{-2} the system is at or near the limiting c.d. for gold discharge and a precipitation of the complex is hardly possible. If the complex could be formed at low c.d. one should observe above 50 mA cm^{-2} a drastic change in the ratio C/Co and Co/Au in the deposit, which is not the case. In fact, the atomic ratio varies over a wide range depending on the plating conditions. Table 2 summarizes the values found by us and other authors. In view of the large scatter displayed in Table 2 it must be concluded that no well-defined single compound is present in major portions in the deposit, especially as far as carbon and cobalt are concerned. However, the formation of some complicated mixture depending on the conditions cannot be excluded.

Let us now consider more particularly the incorporation of carbon. According to Holt and Stanyer [31] and Raub *et al.* [42] who used a tracer technique, the carbon in the deposit originates in the cyanide and not in the citrate of the bath. It has been speculated that it comes from a cobalt cyanide complex in the solution. In fact, one does not know very well which is the predominant cobalt complex present in the DUOR bath. In any case, the ratios C/Co reported in Table 2 show that the carbon must come, at least to a large extent, from the gold cyanide. This is substantiated by a comparison of Figs. 5b and 9b. The rate of incorporation of carbon and gold deposition are seen to change with the conditions in a similar way. The above conclusion is also in agreement with the result of the kinetic studies of Harrison and Thompson [18] that Au(CN) is adsorbed on the surface prior to the gold discharge. We can thus envisage, as a very rough model, the following mechanism. Gold is first adsorbed as Au(CN). It can then be decomposed in two ways: (a) after discharge of the gold complex the cyanide formed is recycled into the solution where it further reacts to HCN; (b) the cyanide undergoes, at the metal surface, a reaction involving hydrogen and leading at least partially to an incorporation of the products into the deposit. The involvement of hydrogen is suggested by the following facts. When cobalt is added to the solution carbon and hydrogen appear simultaneously in the deposit. When the pH of the solution is increased the carbon content of the deposit and the current efficiency for hydrogen evolution strongly decreases (above pH 5). A noteworthy link between current efficiency and carbon content has also been observed in the experiments with pulse electrolysis. We will come back to this point in a later paper [7].

8. Practical implications

From the technical viewpoint the most relevant fact is that the porosity, which is of importance for the corrosion resistance, substantially decreases with decreasing current density and increasing flow rate. By and large the porosity seems to increase when the ratio j_{Au} to the limiting current of gold deposition increases. At the usual operating conditions of technical gold baths (10 mA

cm^{-2}, agitation predominantly by gas evolution) this ratio is probably about 0·3–0·4 whereas the rate of cobalt incorporation is close to or at its limiting rate (where it has been assumed that the mass transport coefficients in the technical baths are approximately the same as those in our experiments at $(Re) = 2900$, see Figs. 5a and 10).

Acknowledgements

The financial support by Flühmann and Co., Zurich/Dübendorf, Switzerland is gratefully acknowledged. Thanks are due to Dr H. Feichtinger (Institute for Metallurgy, Professor Dr B. Marincek, ETH) for his help with the carbon determination as well as to Dr Magyar (Department of Inorganic Chemistry, ETH) and to Mr Esenwein (EMPA Dübendorf) for carrying out the cobalt analysis.

References

[1] D. Lloyd-Jacob, *Gold Bull.* **4** (1971) 25.
[2] F. H. Reid, *ibid,* **6** (1973) 77.
[3] *Ibid,* **5** (1972) 85.
[4] M. Antler, *ibid,* **4** (1971) 42.
[5] N. Ibl, J. Cl. Puippe and H. Angerer, Paper presented at *the 28th ISE Meeting in Druzhba (Bulgaria) (1977).*
[6] *Idem, Surface Techn.* **6** (1978) 287.
[7] H. Angerer and N. Ibl, in preparation.
[8] A. Knödler, *Metalloberfläche* **28** (1974) 465.
[9] E. N. Wiese, P. W. Gilles and C. A. Reynolds, *Analyt. Chem.* **25** (1953) 1344.
[10] M. Clarke and J. M. Leeds, *Trans. Inst. Met. Finishing* **43** (1965) 54.
[11] *Idem, ibid,* **46** (1968) 81.
[12] H. Angerer, thesis in preparation, Swiss Federal Institute of Technology (1978).
[13] T. Mizuskina in 'Advances in Heat Transfer' Vol. 7, (edited by T. F. Irvine) Academic Press, (1977) pp. 87–161.
[14] D. J. Pickett and K. L. Ong, *Electrochim. Acta* **19** (1974) 875.
[15] H. Y. Cheh, *J. Electrochem. Soc.* **118** (1971) 551.
[16] V. G. Levich, *Acta Physiochim. USSR* **17** (1942) 257.
[17] I. A. Kakovskii, A. N. Lebedev and O. K. Sheberbakov, *Chem. Abstr.* **69** (1968) 99 994.
[18] J. A. Harrison and J. Thompson, *J. Electroanalyt. Chem.* **40** (1972) 113.
[19] I. R. Burrows, J. A. Harrison and J. Thompson, *ibid,* **53** (1974) 283.
[20] N. Ibl in 'Treatise on Electrochemistry', Vol. III, (edited by E. Yeager, J. O'M. Bockris and B. Conway) Ch. 1.
[21] N. Ibl and J. Venczel, *Metalloberfläche* **24** (1970) 365.
[22] N. Ibl, *Chem. Ing. Techn.* **43** (1971) 202.
[23] H. Vogt, *Electrochim. Acta* **23** (1978) 203.
[24] Landolt-Börnstein, Zahlenwerte und Funktionen, 5. Teil, Bandteil a (Transportphänomene I), Springer–Verlag (1969).
[25] M. Clarke, *Trans. Inst. Met. Finishing* **51** (1973) 150.
[26] J. M. Leeds and M. Clarke, *ibid,* 47 (1969) 163.
[27] K. G. Ashurst and R. W. Neale, *ibid,* **45** (1967) 75.
[28] T. F. Egan, *Microchem. J.* **24** (1968) 646.
[29] G. B. Munier, *Plating* **56** (1969) 1151.
[30] L. Holt, P. J. Ellis and J. Stanyer, *ibid,* **60** (1973) 910, 918.
[31] L. Holt and J. Stanyer, *Trans. Inst. Met. Finishing* **50** (1972) 24.
[32] L. Holt, *ibid,* **51** (1973) 134.
[33] N. Ibl, 'Advances in Electrochemistry and Electrochemical Engineering', Vol. 2 (edited by P. Delahay and C. W. Tobias) Interscience New York (1962) p. 49.
[34] *Idem, J. Electrochem. Soc.* **114** (1967) 1268.
[35] *Idem, Proceedings Corrosion Metal Finishing, International Conference* Basle (1966) Forster Verlag, Zürich, p. 48.
[36] A. R. Despic and Y. I. Popov, *Mod. Aspects Electrochem.* **7** (1977) 199.
[37] D. L. Malme and M. J. Vasile, *J. Electrochem. Soc.* **120** (1973) 1484.
[38] Ch. J. Raub, A. Knödler and J. Lendvay, *Plating* **63** (1976) 35.
[39] H. G. Silver, *J. Electrochem. Soc.* **116** (1969) 591.
[40] O. J. Hüttner and R. C. Sanwald, *Plating* **59** (1972) 750.
[41] E. T. Eisenmann, *J. Electrochem. Soc.* **124** (1977) 1957.
[42] E. Raub, Ch. J. Raub, A. Knödler and H. P. Wiehl, *Werkstoffe und Korrosion* **23** (1972) 643.
[43] H. Fischer, 'Elektrolytische Abscheidung und Elektrokristallisation von Metallen', Springer–Verlag (1954).
[44] J. Bielinski, unpublished work.